buildings

MDPI

Review

A Review of Evaluation Methods of Standards for Structural Vibration Serviceability under Crowd Walking

Jiecheng Xiong, Zhihao Liu, Shuqian Duan * and Hui Qian

School of Civil Engineering, Zhengzhou University, Zhengzhou 450001, China; xiongjc2019@zzu.edu.cn (J.X.); lzh17319737340@163.com (Z.L.); qianhui@zzu.edu.cn (H.Q.)
* Correspondence: shuqianduan@zzu.edu.cn

Abstract: Structures such as long-span footbridges, floors, and long cantilevers are vulnerable to vibration serviceability problems under crowd walking, which should be taken into consideration during the structural design, operation, and maintenance stages. Standards have been developed to enable designers to assess the vibration serviceability of structures using simplified load models that simulate crowd-induced loading. To facilitate engineers in quickly selecting appropriate standards for vibration serviceability design, ten current standards were collected which deal with the assessment of structural vibration serviceability under walking loads, including the French "Assessment of vibrational behavior of footbridges under pedestrian loading" (2006), the German "Design of footbridges guideline" (2007), the Chinese "Technical standard for human comfort of the floor vibration" (2019), etc. The ten standards were reviewed and evaluated from three aspects including the crowd loading model, structural response calculation method, and vibration serviceability evaluation standard in this paper. Through summary and comparison between standards, three directions for future improvement and perfection of the standards were proposed: the challenges of the improvement of the standards focus on the establishment of the refined stochastic load model, the analysis of the crowd–structure coupling system, and the modelling of multifactor coupling serviceability evaluation indexes.

Keywords: human induced vibration; walking load; standards; vibration serviceability

check for updates

Citation: Xiong, J.; Liu, Z.; Duan, S.; Qian, H. A Review of Evaluation Methods of Standards for Structural Vibration Serviceability under Crowd Walking. *Buildings* **2024**, *14*, 675. https://doi.org/10.3390/buildings14030675

Academic Editor: Ehsan Noroozinejad Farsangi

Received: 8 January 2024
Revised: 26 February 2024
Accepted: 1 March 2024
Published: 3 March 2024

1. Introduction

In recent years, with the continuous improvement of the strength of building materials and the requirements for architectural aesthetics, structures such as building floors and footbridges have been evolving towards lightweight, high-strength, long-span, and flexible designs [1–4]. Such structures exhibit low fundamental frequencies and limited damping, consequently raising concerns regarding vibration serviceability during crowd walking [5]. Since the new century, the most influential incident has undoubtedly been the Millennium Bridge incident in London in 2000 [6]. As a large number of people crossed the bridge on the first day of its opening, the bridge experienced significant vibrations and was forced to close for two years and huge sums of money were spent to install vibration reduction devices. The Jiebai Bridge outside a department store in Hangzhou, which was once the longest-span steel box girder footbridge in China, faced continuous controversy due to its persistent 'swaying' issues, ultimately necessitating its demolition and reconstruction in 2012. The recurrent and widespread nature of the above-mentioned serviceability issues give universal and important significance to the proposition of studying the vibration mechanism and serviceability evaluation of structures under crowd walking, which necessitates significant attention from both scholars and engineers alike [7].

Nowadays, human-induced vibrations are becoming an increasingly important in modern structural design [8]. Unlike earthquakes [9,10], wind loads [11], or other effects [12,13], it is widely acknowledged that vibrations generated by human-induced loads are typically considered a serviceability rather than a safety issue. This is primarily due to the fact that humans are extremely sensitive to vibration levels as low as 0.001 mm [14]. Such heightened sensitivity often leads to the identification of vibration serviceability problems long before the vibration levels reach levels capable of causing structural damage. The majority of reports on these issues indicate that excessive vibrations are typically caused by a near-resonance of one or more vibration modes [15]. This occurs because the natural frequency range of lightweight and slender structures often aligns with the dominant frequencies of human-induced dynamic loads [16–18].

Standards have been developed to enable designers to assess the vibration serviceability of structures using simplified load models that simulate crowd-induced loading. At present, the standards related to the assessment of structural vibration serviceability under walking loads mainly include the French "Assessment of vibrational behaviour of footbridges under pedestrian loading" (2006) (referred to as Sétra) [19], the German "Design of footbridges guideline"(2007) (referred to as EN03) [20], European "Design of bridges: guidebook 2"(2010) (referred to as Guidebook 2) [21], International Federation for Structural Concrete "Guidelines for the design of footbridges" (2005) (referred to as FIB 32) [22], International Organization for Standard "Bases for design of structures—Serviceability of buildings and walkways against vibrations" (2007) (referred to as ISO 10137) [23], British standards "UK National Annex to Eurocode 1: Actions on structures-Part 2: Traffic loads on bridges" (2008) (referred to as BSI) [24], the United States "Floor vibrations due to human activity" (2016) (referred to as AISC) [25], and the Chinese "Technical specification for concrete structures of tall building" (2010) (referred to as JGJ 3) [26], "Technical standard for human comfort of the floor vibration" (2019) (referred to as JGJ/T 441) [27], "Technical specifications of urban pedestrian overcrossing and underpass (Draft for Comments)" (2017) (referred to as CJJ 69) [28]. A systematic procedure is provided for the vibration serviceability assessment by the standards. The relevant research within the standards was carried out in three main directions: crowd load models, calculation of human-induced vibration responses, and standards for evaluating vibration serviceability, covering the three areas of vibration source, propagation path, and vibration response receiver, respectively [29]. The three corresponding research aspects were load models, structural vibration analysis methods, and criteria of vibration serviceability, respectively. This review is intended to provide a critical overview of the ten standards that deal with the vibration serviceability under crowd walking. By comprehensively summarizing the standards from the three aforementioned aspects, we can identify the current advantages and disadvantages in the standards. Additionally, we seek to highlight the challenges encountered in enhancing and refining these standards.

2. Walking Load

Walking load corresponds to the vibration source of human-induced vibration problems and is the basis for human-induced vibration serviceability evaluation of structures [30]. Therefore, establishing a reliable walking load model is the prerequisite for accurately predicting the structural vibration response under the action of crowd [31]. During human walking, there is a repetitive process of the alternating contact of the heels and lifting of the toes in the forward direction, so the walking load is approximately periodic and contains three components: vertical, horizontal, and longitudinal [32]. For structures with weak horizontal constraints such as pedestrian bridges, the vertical and horizontal components of the load easily trigger structural vibrations [33]. Conversely, for structures with strong horizontal constraints like floors, the vertical component tends to induce structural vibrations [34,35]. Consequently, current research on walking loads mainly focuses on the vertical and horizontal components.

2.1. Fourier Series Model

Regardless of the vertical load component or the horizontal load component, except for JGJ3, which does not provide a specific load model, the other nine standards use Fourier series model to represent the approximate periodicity of the load [36]:

$$F(t) = C\left(G + \sum_{i=1}^{n} G\alpha_i \sin(2n\pi f t - \varphi_i)\right) \tag{1}$$

where G is the static weight of the pedestrian, α_i is the Fourier coefficient of the ith harmonic (generally known as the dynamic loading factor), f is the step frequency, φ_i is the phase shift of the ith harmonic, and C is the amplification factor of crowd load. Each standard establishes dynamic loading factor and amplification factor models under different working conditions through measured load data fitting and structural response simulation. The values of vertical load and horizontal load model parameters are shown in Tables 1 and 2, respectively.

Table 1. Values of Fourier model parameters for vertical loads.

Standards	Amplification Factor	Dynamic Loading Factor	Phase Shift	Weight	Load Type	Structures
Sétra [19]	$n' \times \psi$ m^{-2}	$\alpha_1 = 0.4$, $\alpha_2 = 0.1$	$\varphi_1 = \varphi_2 = \pi/2$	G = 700 N	uniform	Footbridges
EN03 [20]	$n' \times \psi$ m^{-2}	$\alpha_1 = 0.4$, $\alpha_2 = 0.1$	$\varphi_1 = \varphi_2 = \pi/2$	G = 700 N	uniform	Footbridges
CJJ 69 [28]	$n' \times \psi$ m^{-2}	$\alpha_1 = 0.4$	$\varphi_1 = \pi/2$	G = 700 N	uniform	Footbridges
JGJ/T441 [27]	$10.8\sqrt{\frac{\xi}{25}} \times \psi$ m^{-2}	$\alpha_1 = 0.4$, $\alpha_2 = 0.1$	$\varphi_1 = \pi/2$	G = 700 N	uniform	Corridors and indoor bridges
Guidebook 2 [21]	$k_v(f_v)$ -	$\alpha_1 = 0.257$	$\varphi_1 = 0$	G = 700 N	concentrate	Footbridges
	$15\, k_v(f_v)$ m^{-2}	-	$\varphi_1 = 0$	-	uniform	Footbridges
FIB 32 [22]	$k_v(f_v)$ -	$\alpha_1 = 0.257$	$\varphi_1 = 0$	G = 700 N	concentrate	Footbridges
	$12.6\, k_v(f_v)$ m^{-2}	-	$\varphi_1 = 0$	-	uniform	Footbridges
BSI [24]	$k\sqrt{1+\gamma(N-1)}$ -	$\alpha_1 = 0.4$	$\varphi_1 = 0$	G = 700 N	concentrate	Footbridges
	$1.8\frac{k}{A}\sqrt{\frac{\gamma\rho A}{\lambda}}$ m^{-2}	$\alpha_1 = 0.4$	$\varphi_1 = 0$	G = 700 N	uniform	Footbridges
ISO 10137 [23]	$\sqrt{N}$ -	$\alpha_1 = 0.37(f-1.0)$, $\alpha_2 = 0.1\alpha_3 = 0.06$, $\alpha_4 = 0.06, \alpha_5 = 0.06$	-	G = 750 N	concentrate	Walkways
AISC [25]	-	$\alpha_1 = 0.5$, $\alpha_2 = 0.2, \alpha_3 = 0.1$, $\alpha_4 = 0.05$	$\varphi_1 = \pi/2$	G = 700 N	concentrate	Floors
JGJ3 [26]	-	-	-	-	-	-

Table 2. Values of Fourier model parameters for horizontal loads.

Standards	Amplification Factor	Dynamic Loading Factor	Phase Shift	Weight	Load Type	Structures
Sétra [19]	$n' \times \psi$ m^{-2}	$\alpha_1 = 0.05$	$\varphi_1 = \pi/2$	G = 700 N	uniform	Footbridges
EN03 [20]	$n' \times \psi$ m^{-2}	$\alpha_1 = 0.05$	$\varphi_1 = \pi/2$	G = 700 N	uniform	Footbridges
CJJ 69 [28]	$n' \times \psi$ m^{-2}	$\alpha_1 = 0.05$	$\varphi_1 = \pi/2$	G = 700 N	uniform	Footbridges
JGJ/T441 [27]	$10.8\sqrt{\frac{\xi}{25}} \times \psi$ m^{-2}	$\alpha_1 = 0.05$	$\varphi_1 = \pi/2$	G = 700 N	uniform	Corridors and indoor bridges
Guidebook 2 [21]	$k_h(f_h)$ -	$\alpha_1 = 0.1$	$\varphi_1 = 0$	G = 700 N	concentrate	Footbridges
	$4\, k_h(f_h)$ m^{-2}	-	$\varphi_1 = 0$	-	uniform	Footbridges
FIB 32 [22]	$k_h(f_h)$ -	$\alpha_1 = 0.1$	$\varphi_1 = 0$	G = 700 N	concentrate	Footbridges
	$3.2\, k_h(f_h)$ m^{-2}	-	$\varphi_1 = 0$	-	uniform	Footbridges
BSI [24]	-	-	-	-	-	-
ISO 10137 [23]	$\sqrt{N}$ -	$\alpha_1 = 0.1$	-	G = 750 N	concentrate	Walkways
AISC [25]	-	-	-	-	-	-
JGJ3 [26]	-	-	-	-	-	-

Sétra is well-suited for the design and assessment of footbridges, treating pedestrians load as a deterministic load (N/m^2) uniformly distributed across the bridge deck. It employs a cosine wave load model to calculate the human-induced vibrations response and is applied to the structure for a particular mode shape. Additionally, both the vertical and horizontal walking loads consistently account for the first second-order dynamic load factors. The load model used in EN03 is similar to Sétra's, but the horizontal walking load exclusively takes into account the first-order dynamic load factor. Among them, the crowd amplification factor is obtained by multiplying the equivalent crowd density and the non-resonant reduction factor ψ. n' is the ratio of the fully synchronized equivalent crowd to the effective area of the bridge deck, which is obtained through structural response simulation and is defined such that the same acceleration level is generated as the 95 percentile-value of the peak accelerations of 500 simulated streams of n random pedestrians [37]. Various crowd densities were differentiated throughout the simulation process, leading to the development of a corresponding calculation formula (Equation (2)) for the equivalent crowd density model. The non-resonance reduction factor ψ takes into account the reduction of the structural response when the structural frequency falls outside the frequency range of the walking load. The Chinese standards CJJ 69 and JGJ/T441 are specifically intended for the design of footbridges, corridors, and indoor bridges, with the load model referring to EN03. Notably, the values for the non-resonance reduction coefficient (see Figure 1), equivalent crowd density, and model harmonics differ across these four aforementioned standards (detailed in Tables 1 and 2).

$$n' = \begin{cases} 10.8\sqrt{\frac{\xi \times d}{S}} & d < 1.0\,\text{person/m}^2 \\ 1.85\sqrt{\frac{d}{S}} & d \geq 1.0\,\text{person/m}^2 \end{cases} \tag{2}$$

where ξ is the structural damping ratio, S is the effective area of the bridge.

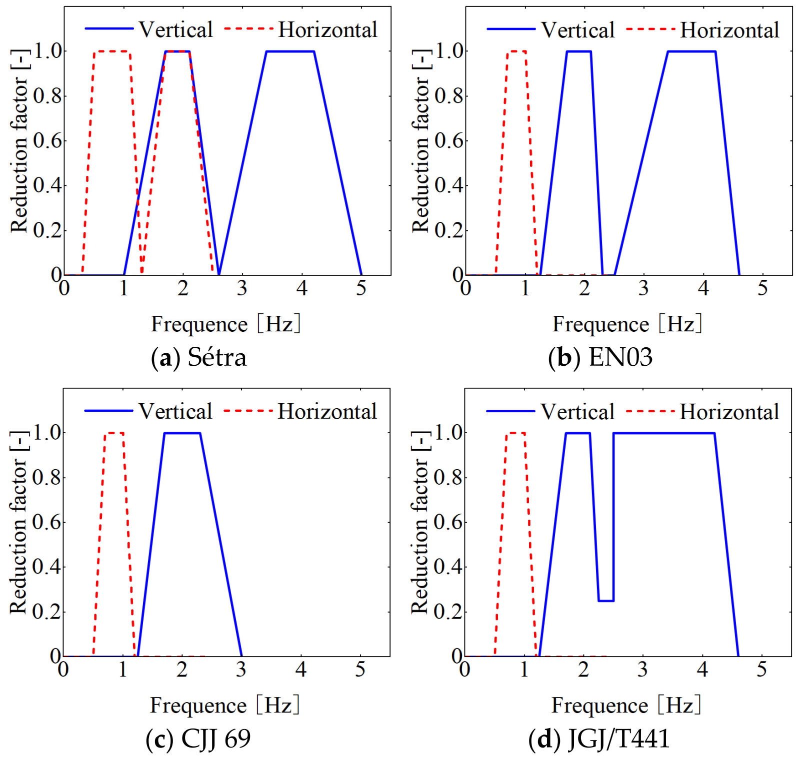

Figure 1. Values of non-resonant reduction factors [19,20,27,28].

Guidebook 2 and FIB 32 are used for footbridges, sharing similar crowd load models that categorize walking patterns based on pedestrian numbers as group of pedestrians and continuous pedestrian steam. In reality, the process of a crowd crossing a bridge is highly complex. The crowd can be seen as a multi-point excitation model, with the position of action points varying due to pedestrian movement [38]. Currently, there is no load model that adequately considers the mobility and multi-point properties of this phenomenon. To aid in structural design, 8–15 pedestrians walking together is defined as group of pedestrians walking, which is represented as a concentrated force positioned at the bridge deck's most critical location (usually the point of maximum vibration). This approach transforms a multi-point model into a single-point model and does not consider mobility under a conservative assumption. Similarly, high-density crowds walking, exceeding 15 individuals, or with a density greater than 0.6 persons/m^2, are defined as continuous pedestrian steam. Here, pedestrians are uniformly distributed on the bridge with consistent spacing between individuals, same as Sétra, which adopts uniformly distributed load representations in its load model. Among the model parameters, the vertical load crowd amplification factor ($k_v(f_v)$) of the two standards has different values, while the horizontal load crowd amplification factor ($k_h(f_h)$) is the same, as shown in Figure 2. f_v and f_h are the vertical and horizontal natural frequencies of the structure, respectively.

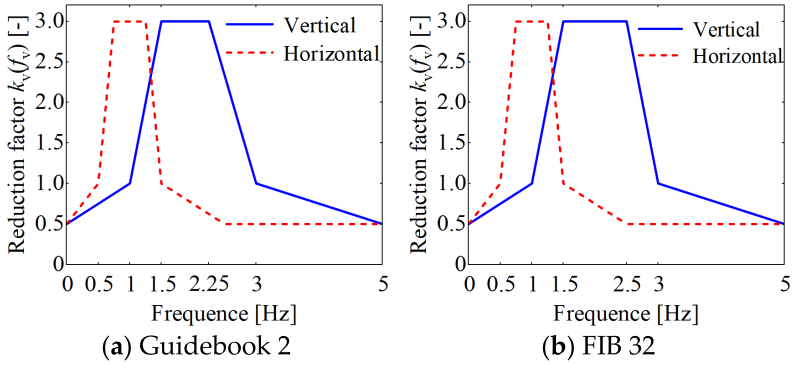

Figure 2. Values of magnification factors for the crowd load [21,22].

The BSI is also designed for footbridges, resembling the depiction of pedestrian walking activities found in Guidebook 2 and FIB 32. It mirrors the representation of group of pedestrians walking as concentrated force and continuous pedestrian steam walking as a uniform load. Unlike the former references, this code lacks a specific model for horizontal load. Within Table 1, N and ρ denote the number and density of pedestrians, respectively. During the design phase, the selection between a concentrated force model or a uniform distributed load model depends on the actual circumstances, guided by recommended values listed in Table 3 below. Within the model, λ stands for the coefficient associated with population distribution, conservatively set at 0.634. The parameter k relates to the structure's frequency, which accounts for the impact of pedestrian numbers, harmonic responses, and the relative weight of pedestrian sensitivity responses. Additionally, γ serves as a reduction coefficient accommodating the out-of-synchrony phenomenon between pedestrians and relates to the structural damping ratio.

Table 3. Recommended crowd sizes and densities for design.

Bridge Usage	Group Size	Crowd Density
Rural locations seldom used and in sparsely populated areas.	$N = 2$	$\rho = 0$ person/m^2
Suburban location likely to experience slight variations in pedestrian loading intensity on an occasional basis.	$N = 4$	$\rho = 0.4$ person/m^2
Urban routes subject to significant variation in daily usage (e.g., structures serving access to offices or schools)	$N = 8$	$\rho = 0.8$ person/m^2
Primary access to major public assembly facilities such as sports stadia or major public transportation facilities.	$N = 16$	$\rho = 1.5$ person/m^2

The ISO 10137 accounts for the first five-order dynamic load factors for vertical walking load and the first-order dynamic load factors for lateral walking load. This standard find application in calculating various walkways, including footbridges, indoor corridors, and floor walkways. Exploring the crowd load amplification factor C, assuming uniform distribution of walking frequencies and phases between $[0, 2\pi]$ among individuals, the relationship between C and the number of people N is derived as per random vibration theory, yielding $\sqrt{N}$.

The AISC and JGJ3 standards are used for analyzing human-induced vibrations in floors, focusing solely on vertical vibrations. AISC outlines the first four-order dynamic load factors for vertical walking load but does not include the crowd amplification factor. JGJ3 highlights the importance of assessing floor vibration serviceability under walking load effects and offers formulas for structural response calculation along with floor vibration acceleration limits. However, JGJ3 does not specify a particular load model.

2.2. Comparison of Load Models

It can be seen from the above that the values of the crowd load model are related to walking frequency f, crowd density d, structural damping ratio ξ, and other parameters. Therefore, this paper takes the most common case f = 2 Hz, d = 1.0 person/m^2, ξ = 0.01, and calculates the time history curve of the crowd load model. The results are depicted in Figure 3. We present the results of concentrated load and uniform load separately. Notably, the calculation curves for Sétra and EN03 are the same whether it is a concentrated load or a uniform load. However, some load curves exhibit differences in amplitude, number of peaks, mean value, and curve shape, such as BSI and ISO 10137. These disparities are attributed to the orders, dynamic load factor (DLF) values, standard weights, and phase angles of each model. Such discrepancies can be attributed to the different ethnic populations studied across different regions [39]. The standards originate from various countries and regions, with their dynamic load factors derived from load test results conducted by different researchers. This highlights the importance for designers to select appropriate standards for structural design based on the region.

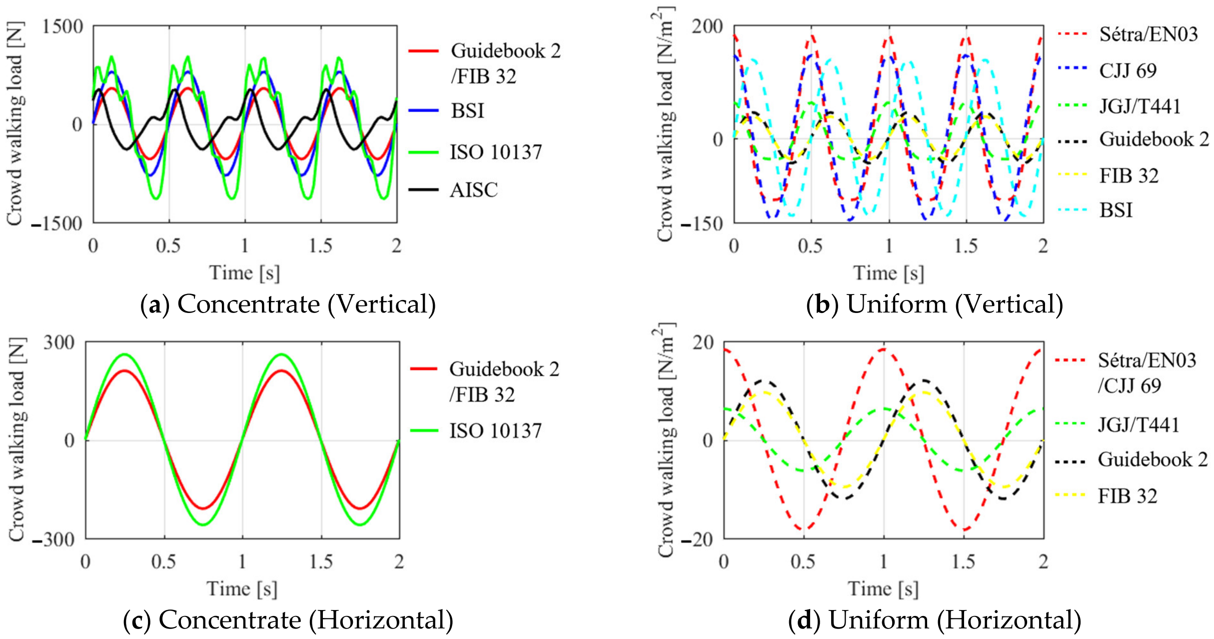

Figure 3. Crowd load time histories of Fourier series load models [19–25,27,28].

2.3. Summary of Load Model

The Fourier series model is widely used in various specifications due to its simple form. In practical applications, the dynamic load factor and crowd amplification factor can be determined based on factors like crowd density and structural frequency. Subsequently, a time history analysis of the structure can be conducted to predict its response. However, the Fourier series model in current specifications typically encounters the following four main issues:

(1) The Fourier series model assumes load energy concentrates solely at the primary frequency and its multiples, neglecting energy distributed around these frequencies. Consequently, it overlooks the energy present around the main frequency and its multiples,

resulting in significant errors in calculated structural responses, particularly evident at higher-order load harmonics. Chen et al. [40] proposed a power spectrum-density for walking load based on 1528 continuous walking-load time histories. They discovered prominent peaks at both the main harmonic and subharmonic, as well as an energy diffusion phenomenon.

(2) The dynamic load factor and crowd load amplification factor are typically derived as mean values or specific quantiles by fitting measured load data and simulating structural responses. However, these factors overlook the inherent randomness of walking loads, limiting the feasibility of conducting reliability-based serviceability design or structure evaluations.

(3) The crowd walking load exhibits multi-point excitation and movement characteristics. However, the modelling approach for dynamic load factor and crowd load amplification factor simplifies this load into a fixed-point load with single-point excitation [41]. Consequently, the vibration caused by individual steps is disregarded in calculating the structural response. The specification lacks discussion on this specific value type and its influence on structural vibration response.

(4) The oversight of considering structural vibration's impact on crowd loads is notable. Studies indicate pedestrians are less sensitive to vertical structure vibration but more attuned to horizontal vibration [42]. Consequently, the dynamic load factor of lateral walking load and the crowd load amplification factor are influenced by structural vibration. Regrettably, this phenomenon remains unaddressed in the current standards.

3. Calculation of Human-Induced Vibration Responses

Currently, the recommended methods outlined in the standards for calculating the response of structures under walking load primarily consist of the simplified formula method, time history analysis method, and response spectrum method.

3.1. Simplified Formula

The simplified formula method typically assumes the structure to be a single-degree-of-freedom system operating in resonance. It derives the peak acceleration at the structural maximum amplitude through the equation of motion. Table 4 presents the structural response simplified formulas outlined in the aforementioned ten standards.

Table 4. Formula of structural acceleration amplitude.

Standards	Formulas	Structures	Description of Parameters
Sétra [19]	$a_{\max} = \frac{1}{2\xi}\frac{4F}{\pi\rho S}$	Footbridges	$a_{\max}$ is the acceleration of the most unfavorable point of the structure, F is the amplitude of the force per unit length, ξ is the structural damping ratio, ρ is the density of structure, S is the effective width of bridges
EN03 [20]	$a_{\max,n} = \frac{1}{2\xi}\frac{p_n}{m_n}$	Footbridges	$a_{\max,n}$ is the modal acceleration, p_n is the generalized load, m_n is the generalized (modal) mass
CJJ 69 [28]	Same as EN03	Footbridges	Same as EN03
JGJ/T441 [27]	Same as AISC	Floors	Same as AISC
Guidebook 2 [21]	$a_{\max} = 165k_{\mathrm{v}}(f_{\mathrm{v}})\frac{1-\exp(-2n\pi\xi)}{M\xi}$	Footbridges	M is the total mass of the bridge, n is the number of steps to cross the span, $k_{\mathrm{v}}(f_{\mathrm{v}})$ is the crowd amplification factor
FIB 32 [22]	$a_{\max} = S \cdot 0.6F\frac{1-\exp(-2n\pi\xi)}{M\xi}$	Footbridges	S is the crowd amplification factor, F is the amplitude of the force, n is the number of steps to cross the span
BSI [24]	-	-	-
ISO 10137 [23]	-	-	-
AISC [25]	$a_{\max} = \frac{P_0\exp(-0.35f_n)}{\xi W}g$	Floors	W is the effective weight of the floor, p_0 is the constant force of people, ξ is the damping ratio of floor, f_n is the natural frequency of floor, g is the acceleration of gravity
JGJ3 [26]	Same as AISC	Floors	Same as AISC

Sétra adopts the most conservative loading approach, aligning the uniform load's direction with the vibration direction. It derives the acceleration amplitude of footbridge structures under crowd walking based on resonance assumption. In this context, the unit force amplitude F is obtained from load model amplitude from Table 1 or Table 2 is acquired by multiplying the effective width of the bridge. EN03 follows a similar method to determine the acceleration amplitude of footbridge structures under crowd walking. It involves obtaining the generalized mass and load by multiplying the mode shape with the mass and load, respectively. The acceleration calculation outcomes depend on the structural damping ratio. Both codes offer recommended damping ratio values for various structure types, detailed in Table 5. CJJ 69 also adopts the structural response formula outlined in EN03.

Table 5. Damping ratios for different construction types (%).

Construction Types		Reinforced Concrete	Prestressed Concrete	Composite Steel–Concrete	Steel	Timber	Stress-Ribbon
Sétra [19]	Min	0.8	0.5	0.3	0.2	1.5	-
	Mean	1.3	1.0	0.6	0.4	3.0	-
EN03 [20]	Min	0.8	0.5	0.3	0.2	1.0	0.7
	Mean	1.3	1.0	0.6	0.4	1.5	1.0

Guidebook 2 also relies on the calculation formula for vertical acceleration responses due to crowd movement on a simply supported girder bridge. The value 'n' equals the bridge span divided by the step length. The load crowd amplification factor $k_{\mathrm{v}}(f_{\mathrm{v}})$ is determined from the recommended load model illustrated in Figure 2a within the standard. FIB 32 involves multiplying the crowd response amplification factor 'S' with the acceleration induced by a single person on a simply supported girder bridge to obtain the peak acceleration at the most critical bridge position under crowd loading. 'S' correlates with the structural frequency and is calculated under the following two scenarios:

(1) Group of pedestrians walk through the bridge:

$$S = \begin{cases} 1 & 0\,\mathrm{Hz} < f \leq 1.0\,\mathrm{Hz} \\ 4f - 3 & 1.0\,\mathrm{Hz} < f \leq 1.5\,\mathrm{Hz} \\ 3 & 1.5\,\mathrm{Hz} < f \leq 2.5\,\mathrm{Hz} \\ -3f + 10.5 & 2.5\,\mathrm{Hz} < f \leq 3.0\,\mathrm{Hz} \\ 1.5 & 3.0\,\mathrm{Hz} < f \leq 5.0\,\mathrm{Hz} \end{cases} \tag{3}$$

(2) Continuous pedestrian steam walk through the bridge:

$$S = \begin{cases} 0.225N_r & 1.5\,\mathrm{Hz} < f \leq 2.5\,\mathrm{Hz} \\ \sqrt{N_r} & 2.5\,\mathrm{Hz} < f \leq 3.5\,\mathrm{Hz} \\ 0.225 \cdot 0.5 \cdot N_r & 3.5\,\mathrm{Hz} < f \leq 4.5\,\mathrm{Hz} \end{cases} \tag{4}$$

$$N_r = qLb_{\mathrm{eff}}K \tag{5}$$

where f is the structural frequency, N_{r} is the number of pedestrians on the bridge, q is the density of pedestrian, $\mathrm{b}_{\mathrm{eff}}$ is the effective width of the bridge, and K is equal to 0.6.

AISC derived the formula to calculate the maximum acceleration of a floor experiencing the load of a single person walking by correlating frequency and dynamic load factor. The effective weight 'W' is associated with the span and effective width of the floor; a detailed explanation is beyond the scope here. For an in-depth calculation methodology, please refer to Chapter 4 of the standard. The Chinese standards JGJ3 and JGJ/T441 employ an identical formula to AISC's. However, slight differences exist in the values of force 'P_0' and damping ratio 'ξ' among these three standards, as outlined in Table 6.

Table 6. Human walking forces and structural damping ratios.

Building Types	AISC [25]		JGJ3 [26]		JGJ/T441 [27]	
	P_0 N	ξ	P_0 N	ξ	P_0 N	ξ
Offices, Residences, Churches	290	0.02–0.05	300	0.02–0.05	290	0.05
Shopping Malls	290	0.02	300	0.02	290	0.05
Footbridges—Indoor	410	0.01	420	0.01–0.02	-	-
Footbridges—Outdoor	410	0.01	420	0.01	-	-

An experiment on a footbridge was conducted as described in Reference [31]. Therefore, this paper adopts the simplified formulas from the standards, which were used to calculate the response of footbridges, to predict the structural response. Figure 4 presents the calculation results alongside those from the reference. The comparison demonstrates that the formula from the specification is utilized. The larger predicted value of the simplified formula is due to its consideration of the most unfavorable situation to calculate the maximum acceleration at the most critical position of the structure, making it a conservative method.

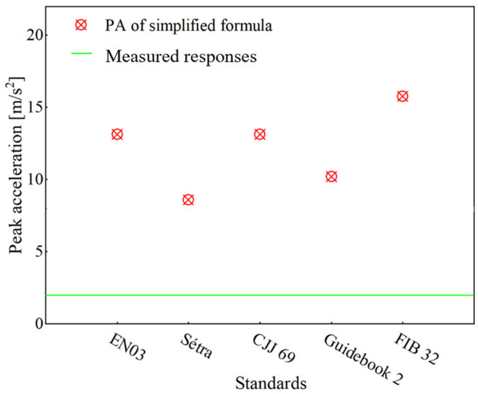

Figure 4. Comparison of predicted results with reference [19–22,28].

3.2. Time History Analysis

Time history analysis method is a numerical approach used to analyze a structural dynamic response in the time domain. It accurately calculates the structural response time history through incremental integration. In addressing human-induced vibration serviceability problems, the load model can simulate crowd load time histories under various conditions. These can then be applied to the structural finite element model or structural motion equation to calculate the structural vibration response time history, facilitating a comprehensive structural serviceability assessment.

3.3. Response Spectrum

The response spectrum serves to depict the peak response of a single-degree-of-freedom system under distinct load excitation, varying with structural frequency and damping ratio. This approach not only accounts for the structure's dynamic properties to a certain extent but also streamlines the structural response into an analytical representation. This method draws inspiration from the widespread use of response spectra in seismic analysis of structures. In recent years, some researchers have tried to integrate this technique into the analysis of human-induced vibrations in flexible structures [43–45].

EN03 assumes the footbridge structure to be a single-degree-of-freedom system, with its mode shape represented as a sinusoidal curve. The task involves deriving the response spectrum for the 95th percentile peak acceleration of the structure under pedestrian flow:

$$a_{\max,95\%} = k_{a,95\%}\sqrt{k_1 \xi^{k_2} \frac{C k_F^2 n^2}{{m_i}^2}} \quad (6)$$

where $k_{a,95\%}$ is the peak factor with 95% guarantee, m_i is the modal mass of the considered mode I, ξ is the structural damping ratio, C is the constant describing the maximum of the load spectrum, n is the number of pedestrians on the bridge, k_F is a constant, and k_1 and k_2 are coefficients related to the structural frequency f_i, calculated according to the following formula:

$$\begin{cases} k_1 = a_1 f_i^2 + a_2 f_i + a_3 \\ k_2 = b_1 f_i^2 + b_2 f_i + b_3 \end{cases} \tag{7}$$

where a_1, a_2, a_3, b_1, b_2, and b_3 are constants detailed in Table 7.

Table 7. Constants for vertical and horizontal accelerations.

Density	Direction	k_F	C	a_1	a_2	a_3	b_1	b_2	b_3	$k_{a,95\%}$
$d \leq 0.5$	Vertical	1.20×10^{-2}	2.95	−0.07	0.60	0.075	0.003	−0.040	−1.000	3.92
	Horizontal	2.85×10^{-4}	6.8	−0.08	0.50	0.085	0.005	−0.06	−1.005	3.77
$d = 1.0$	Vertical	7.00×10^{-3}	3.70	−0.07	0.56	0.084	0.004	−0.045	−1.000	3.80
	Horizontal	2.85×10^{-4}	7.9	−0.08	0.44	0.096	0.007	−0.071	−1.000	3.73
$d = 1.5$	Vertical	3.34×10^{-3}	5.10	−0.08	0.50	0.085	0.005	−0.060	−1.005	3.74
	Horizontal	2.85×10^{-4}	12.6	−0.07	0.31	0.120	0.009	−0.094	−1.020	3.63

JGJ/T441 referenced findings from the literature [43] and introduced the acceleration response spectrum for floor structures subjected to the load of a single person walking. This method initially provides the standard 10 S root mean square (rms) acceleration response spectrum $\alpha(f, \xi)$ for the unit modal mass of the structure under a weight-normalized single-person walking load, as depicted in Figure 5. Here, f represents the vertical frequency of the floor, and ξ is the structural damping ratio. Taking into account the coupling effect of modes between the excitation point and the verification point, the calculation formula (Equation (8)) for the 10 S-rms acceleration response ($a_{j\mathrm{rms}}$) corresponding to the jth-order mode shape at the floor verification point is established.

$$a_{j\mathrm{rms}} = \left(1 - e^{-0.1L}\right) \Phi_{wj} \Phi_j \alpha(f, \xi) \frac{P_\mathrm{p}}{M_j} \tag{8}$$

where M_j is the modal mass, L is the span of the floor in the walking direction, $\Phi_{wj}$is the maximum mode shape value along the walking route, $\Phi_j$is the jth mode shape at a specific floor point for the vibration analysis, and P_p is the person's weight, which can be equal to 700 N.

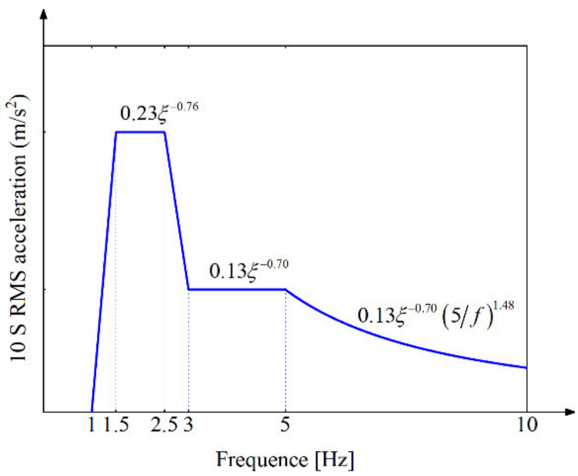

Figure 5. 10 S-RMS acceleration response spectra.

Finally, the maximum value of $a_{j\mathrm{rms}}$ corresponding to each order of modal shape is taken as the root mean square acceleration response a_{rms}. If the peak acceleration a_{p} is used as the index, it can be calculated by Equation (9).

$$a_{\mathrm{p}} = 2a_{\mathrm{rms}} \tag{9}$$

3.4. Summary of Response Calculation Methods

(1) The simplified formula method offers a straightforward calculation model enabling rapid prediction of structural responses. However, its reliance on the single-mode resonance assumption and specific modal shape presumptions during derivation limits its applicability to non-resonant conditions. Moreover, the model's suitability for structures featuring intricate modal shapes or densely packed modes remains unverified.

(2) The time history analysis method excels in providing comprehensive and accurate predictions of structural responses given the load model and structural parameters. However, its drawback lies in its extensive consumption of computing resources and time, particularly during the design phase when structural schemes undergo frequent alterations [43].

(3) The response spectrum method offers swift and precise calculations as its main advantage. However, it is constrained by its applicability to specific structures. If the dynamic properties of the actual structure deviate significantly from those reflected in the derived response spectrum, the utility of this method becomes limited.

(4) The challenge in calculating structural response resides in quantifying the influence of crowds on structural dynamic properties. Crowds possess stiffness, mass, and damping properties, which will change the structural natural frequency and damping ratio [46]. Presently, only Sétra and EN03 address changes in natural frequency resulting from crowd mass, while ISO 10137 suggests that crowds augment structural damping. However, across the simplified formula, time history analysis, and response spectrum methods, there is a deficiency in providing a quantitative depiction of this phase.

4. Vibration Serviceability Evaluation Criteria

The prevailing standards for assessing structural vibration serviceability encompass primarily two methods: the frequency limit method and the acceleration limit method. The frequency limit method regulates the structure's inherent vibration frequency, preventing it from coinciding with the resonant frequency range induced by pedestrian movement, which ensures the structure meets serviceability criteria. Meanwhile, the acceleration limit method maintains human serviceability by restricting the overall human-induced vibration acceleration within specified limits throughout the structure's response history.

4.1. Frequency Limit Method

Table 8 exhibits the frequency calculation formulas and associated frequency limits outlined across the aforementioned 10 standards. Sétra proposes a formula for determining a footbridge's natural frequency, setting a requirement for the vertical frequency not to fall below 5 Hz and the horizontal frequency not to dip below 2.5 Hz. EN03 suggests that evaluation of a structure's serviceability should consider vibration response when the vertical frequency spans 1.25 to 4.6 Hz and the horizontal frequency ranges from 0.5 to 1.2 Hz for footbridges. CJJ 69 mandates a minimum vertical frequency of 3 Hz and a horizontal frequency exceeding 1.2 Hz for footbridges. JGJ/T441 delineates frequency limits for floor structures, corridors, and indoor bridges. For floor structures, the first-order vertical natural vibration frequency should not be less than 3 Hz, calculated via the maximum deflection at the mid-span under the floor's weight. Corridors and indoor overpasses should maintain a first-order horizontal natural vibration frequency not less than 1.2 Hz. Guidebook 2 aligns with Sétra's frequency limits but omits a structural frequency calculation formula. While FIB 32, BSI, ISO 10137, and AISC do not specify structural frequency limits, AISC provides a formula for calculating the natural frequency of floor structures. Additionally, JGJ3 mandates a minimum vertical vibration frequency of 3 Hz for floor structures.

Table 8. Frequency limits of standards.

Standards	Frequency Formulas	Description of Parameters	Vertical Limits	Horizontal Limits	Structures
Sétra [19]	$f_n = \frac{n^2\pi}{2L^2}\sqrt{\frac{EI}{\rho S}}$	L is the length of the bridge, n is the modal order, ρ is the density of the structure, S is the width of the structure, EI is the bending stiffness	>5 Hz	>2.5 Hz	Footbridges
EN03 [20]	$f_1 = \frac{1}{2\pi}\sqrt{\frac{K}{M}}$	K is the stiffness, M is the mass	<1.25 Hz or >4.6 Hz	<0.5 Hz or >1.2 Hz	Footbridges
CJJ 69 [21]	-	-	>3 Hz	>1.2 Hz	Footbridges
JGJ/T441 [27]	$f_1 = \frac{C_f}{\sqrt{\Delta}}$	C_f is generally equal to 18–20, Δ is the maximum deflection at mid-span under the weight of the floor	>3 Hz	>1.2 Hz	Vertical limits apply to floor slabs, and horizontal limits apply to corridors and indoor bridges.
Guidebook 2 [21]	-	-	>5 Hz	>2.5 Hz	Footbridges
FIB 32 [22]	-	-	-	-	-
BSI [24]	-	-	-	-	-
ISO 10137 [23]	-	-	-	-	-
AISC [25]	$f_1 = 0.18\sqrt{\frac{g}{\Delta}}$	g is the acceleration of gravity, Δsame as JGJ/T441	-	-	Floors
JGJ3 [26]	-	-	>3 Hz	-	Floors

4.2. Acceleration Limit Method

The assessment of structural vibration serviceability presently relies on representative values derived from the acceleration response time history. These values typically include peak acceleration (PA), root mean square acceleration (RMS), and vibration dose value (VDV). Equations (10) and (11) are utilized for calculating RMS and VDV, respectively [47]. Table 9 provides an overview of the selected representative value types and their corresponding limits across the 10 standards.

$$a_{\mathrm{w,RMS}} = \left[\frac{1}{T}\int_0^T a_{\mathrm{w}}^2(t)dt\right]^{\frac{1}{2}} \tag{10}$$

$$a_{\mathrm{w,VDV}} = \left[\int_0^T a_{\mathrm{w}}^4(t)dt\right]^{\frac{1}{4}} \tag{11}$$

where $a_{\mathrm{w}}(t)$ is the frequency-weighted acceleration time history, where the weighting curve can refer to the specification ISO 2631-1 [47], and T is the duration.

Table 9. Acceleration limits of standards.

Standards	Types	Vertical Limits	Horizontal Limits	Structures
Sétra [19]	PA	<0.5 m/s^2 (max) 0.5–1.0 m/s^2 (mean) 1.0–2.5 m/s^2 (min) >2.5 m/s^2 (unacceptable)	<0.15 m/s^2 (max) 0.15–0.3 m/s^2 (mean) 0.3–0.8 m/s^2 (min) >0.8 m/s^2 (unacceptable)	Footbridges
EN03 [20]	PA	<0.5 m/s^2 (max) 0.5–1.0 m/s^2 (mean) 1.0–2.5 m/s^2 (min) >2.5 m/s^2 (unacceptable)	<0.1 m/s^2 (max) 0.1–0.3 m/s^2 (mean) 0.3–0.8 m/s^2 (min) >0.8 m/s^2 (unacceptable)	Footbridges

Table 9. *Cont.*

Standards	Types	Vertical Limits	Horizontal Limits	Structures
CJJ 69 [28]	PA	$[0, 0.25f^{0.78})$ m/s^2 (optimal) $[25f^{0.78}, \min(0.5f^{0.5}, 0.7))$ 0.25f m/s^2 (qualified) $[\min(0.5f^{0.5}, 0.7), \infty)$ m/s^2 (unqualified)	$[0, 0.1)$ m/s^2 (optimal) $[0.1, 0.15f^{0.5})$ m/s^2 (qualified) $[0.15f^{0.5}, \infty)$ m/s^2 (unqualified)	Footbridges
JGJ/T441 [27]	PA	0.025 m/s^2	-	Operating room
		0.05 m/s^2	-	Residential, office, etc.
		0.15 m/s^2	-	Shopping malls, restaurants
		0.50 m/s^2	-	Ballroom, stands, etc.
		0.20 m/s^2	-	Gym, workshop office
		0.35 m/s^2	-	entertainment equipment area
		0.40 m/s^2	-	Production operation area
		0.15 m/s^2	0.10 m/s^2	Enclosed corridors and indoor bridges
		0.50 m/s^2	0.10 m/s^2	Unenclosed corridors
Guidebook 2 [21]	PA	0.7 m/s^2	0.15 m/s^2	Footbridges
FIB 32 [22]	-	-	-	-
BSI [24]	PA	$a_{\text{limit}} = k_1k_2k_3k_4$ m/s^2 0.5 m/s$^2 \leq a_{\text{limit}} \leq$ 2.0 m/s^2	-	Footbridges
ISO 10137 [23]	RMS	Figure 6a	Figure 6b	Footbridges
	VDV	0.2~0.4 m/s$^{1.75}$ (Less adverse comments)	-	Residential buildings 16 h day
		0.4~0.8 m/s$^{1.75}$ (Adverse comments possible)	-	
		0.8~1.6 m/s$^{1.75}$ (More adverse comments)	-	
		0.13 m/s$^{1.75}$ (Less adverse comments)	-	Residential buildings 8 h night
		0.26 m/s$^{1.75}$ (Adverse comments possible)	-	
		0.51 m/s$^{1.75}$ (More adverse comments)	-	
AISC [25]	PA	Figure 7	-	Footbridges, corridors, floors
JGJ3 [26]	PA	0.07 m/s^2	-	Residential and office ($f \leq$ 2Hz)
		0.22 m/s^2	-	Shopping malls and indoor corridors ($f \leq$ 2Hz)
		0.05 m/s^2	-	Residential and office ($f \geq$ 4Hz)
		0.15 m/s^2	-	Shopping malls and indoor corridors ($f \geq$ 4Hz)

Sétra and EN03 categorize structural vibration serviceability into four levels: ‘max comfortable,’ ‘mean comfortable,’ ‘min comfortable,’ and ‘unacceptable,’ based on footbridge peak acceleration. CJJ 69 outlines three levels—'optimal,' 'qualified,' and 'unqualified'—for footbridge vibration, with division limits linked to the structure's natural vibration frequency. JGJ/T441 aligns comfort requisites with building usage functions, establishing peak acceleration limits accordingly. Guidebook 2 sets the vertical peak acceleration threshold at 0.7 m/s² and the lateral peak acceleration at 0.15 m/s² for structures. JGJ3 associates comfort requirements with building functions and structural fundamental frequencies, establishing peak acceleration limits accordingly. BSI accounts for multiple factors and presents a formula calculating the vertical peak acceleration limit for footbridges, incorporating coefficients such as k_1 (site usage), k_2 (route redundancy), k_3 (structure height), and k_4 (exposure) defaulting to 1.0 for individual engineering projects. The specific values for k_1, k_2, and k_3 are detailed in Table 10.

Table 10. Values of acceleration limit calculation coefficient of BSI.

Bridge Usages	k_1	Route Redundancy	k_2	Bridge Height	k_3
Primary route for hospitals or other high sensitivity routes	0.6	Sole means of access	0.7	>8 m	0.7
Primary route for school, sports stadia, or other high usage routes	0.8	Primary route	1.0	4–8 m	1.0
Major urban centers	1.0	Alternative routes	1.3	<4 m	1.1
Suburban crossings	1.3				
Rural environments	1.6				

The AISC specification adopts multiples of the ISO 2631-2:1989 [48] benchmark curve to establish vertical peak acceleration limits for various building types, as depicted in Figure 7. Furthermore, the standard suggests that the limits can be assumed to range between 0.8 and 1.5 times the recommended values depending on the duration of vibration and the frequency of vibration events for design purposes.

Unlike other standards, ISO 10137 employs root mean square acceleration and vibration dose values to assess the vibration serviceability of footbridge structures. The root mean square acceleration limit adheres to multiples of the ISO 2631-2:1989 benchmark curve and delineates two operational states: pedestrian stationary and pedestrian walking, detailed in Figure 6. Furthermore, if the ratio of peak acceleration to root mean square acceleration exceeds 6, the comfort assessment incorporates the vibration dose value. The limit value for this assessment depends on the environmental type and duration of use.

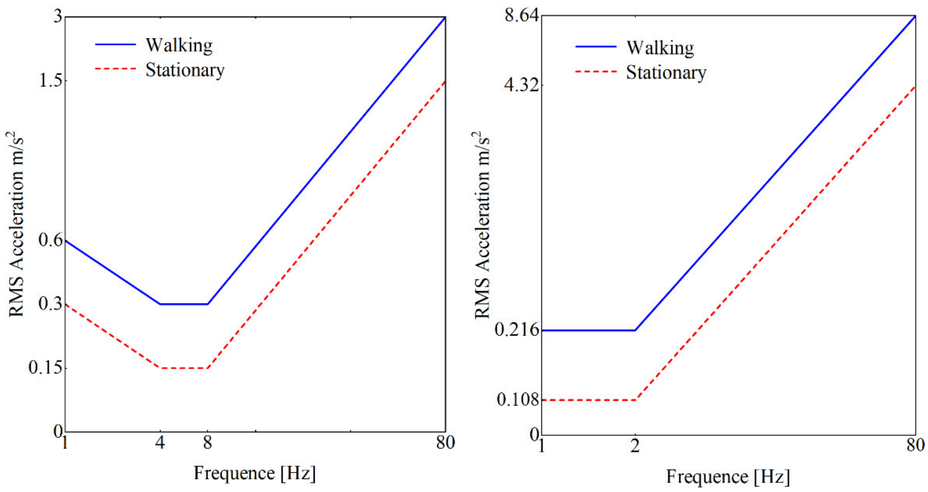

(**a**) Vertical (**b**) Horizontal

Figure 6. RMS limit curves for ISO 10137 [23].

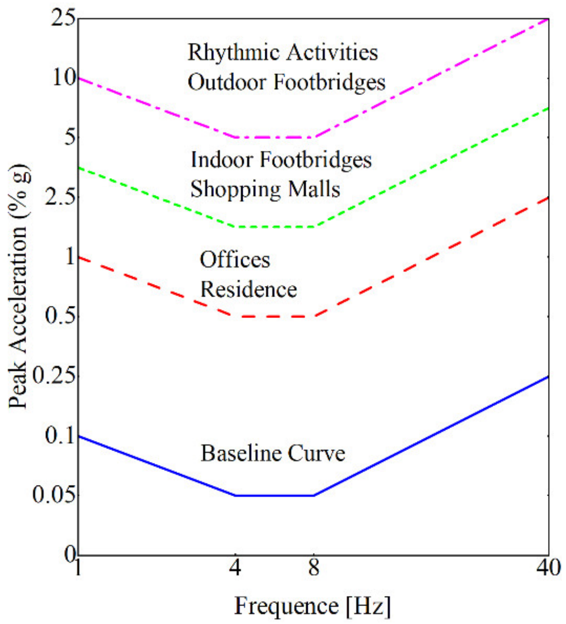

Figure 7. PA limit curves for AISC [25].

4.3. Summary of Vibration Serviceability Criteria

(1) The fundamental frequency of a structure, easily determined through analysis or experimentation, holds clear physical significance, making the frequency limit method straightforward to employ and readily embraced by engineers. However, human serviceability problems arising from structural vibration stem from diverse factors including load history, material composition, structural dimensions, and boundary conditions. Consequently, accurately evaluating structural vibration serviceability solely based on the fundamental frequency of the structure is impractical.

(2) The acceleration limit method comprehensively assesses the amplitude, spectrum, and duration properties of structural vibration, emerging as a leading approach for evaluating structural vibration serviceability. Yet, understanding the human body's response to external vibrations proves intricate, entailing various aspects including the vibration environment and human psychology. Present acceleration limits fail to accurately and quantitatively capture the complex, multi-factor interplay and randomness inherent in these responses. Consequently, conducting reliability-based structural analyses for serviceability design or evaluation remains unfeasible.

5. Discussion

These standards address, to a certain extent, the need for structural vibration serviceability among people. However, with the trend toward longer-span flexible structures in recent years, assessing and designing for structural vibration serviceability will encounter more intricate challenges, demanding extensive and detailed research efforts. In essence, the main points can be summarized as follows:

(1) The establishment of the refined stochastic load model. The statistical modelling of crowd walking loads serves as the foundation for analyzing structural vibration serviceability and is a prerequisite for designing structurally reliable systems [49]. However, current research encounters limitations in mathematically modelling walking load characteristics. There is an overreliance on simplified artificial assumptions, impeding the accurate portrayal of load randomness and spectral components [50]. Recent advancements in high-dimensional data analysis algorithms offer promising avenues for modelling essential walking load characteristics. Envisaging the creation of a high-dimensional probability distribution model encompassing vital features like walking pulses, pulse interval sequences,

and pulse amplitude sequences, there is potential for achieving a more refined and accurate random simulation of crowd walking loads.

(2) The analysis of a crowd–structure coupling system. Recent research on human-induced vibration has highlighted the impact of crowds on the dynamic properties of structures and the reciprocal influence of structural vibration on crowd loads as prominent issues [51]. However, most existing studies have predominantly focused on phenomenological statistical analyses of experimental data, neglecting fundamental physical aspects [52]. Going forward, a promising avenue for exploration involves amalgamating statistical mathematics with physical principles to devise a multi-rigid body mechanical model of the human body. This integration aims to establish a deeper understanding based on certain physical mechanisms [53], representing a worthwhile research direction.

(3) The modelling of multifactor coupled serviceability evaluation indexes. The research on serviceability evaluation indicators involves interdisciplinary studies encompassing biomechanics, psychology, and ergonomics [54]. Current research primarily relies on small-sample phenomenological statistical analyses of indoor experimental data, overlooking the actual human subjective and objective response mechanisms to vibration in real environments, as well as the correlation studies among multiple factors in vibrating environments [55]. The recent advancement in big data technology brings hope for statistical modelling of serviceability evaluation indicators in real vibration environments [56]. It is conceivable that through new methods utilizing big data surveys, there is potential to establish novel, data-rich, multi-factor coupled statistical models for evaluating serviceability. This aims to provide a more robust foundation for reliability-based structural serviceability design and assessment.

6. Conclusions

This review presents a systematic summary of ten standards concerning the assessment of structural vibration serviceability induced by crowd walking. It examines three key aspects: load models, methods for calculating structural vibration responses, and serviceability evaluation criteria. Each standard includes a set of procedures for serviceability evaluation, and while there are similarities, there are also differences between them. Therefore, the main objective of this article is to consolidate the commonly used evaluation methods. This will enable designers to quickly and easily select standards for structural serviceability design, and also signify directions for future enhancements and improvements to the standards.

A multi-order Fourier series deterministic model to represent crowd walking loads is employed in standards, which is a good choice loved by many engineers due to its simplicity. The primary distinction lies in the dynamic load factor's value. Deterministic load models are built on the assumption of forces' perfect periodicity and are derived from force measurements on rigid surfaces. However, human walking is inherently random, and interactions between pedestrians and structures can alter walking patterns. These two facts deserve more attention in future force modelling.

The simplified formula method is primarily relied upon for structural response calculation in the standards. This method involves calculating the maximum acceleration at the most critical position of the structure based on resonance assumptions. During the design phase, engineers can swiftly compute the structural response using its dynamic characteristics to ascertain if it meets vibration serviceability criteria. The use of the response spectrum method in analyzing human-induced vibration in flexible structures enhances the speed and accuracy of the analysis.

As for evaluation of vibration serviceability, the two indicators of frequency and acceleration are adopted. In recent years, there has been a shift away from the frequency limit method towards the acceleration limit method as the standard. This method mainly includes peak acceleration, root mean square value acceleration, and vibration dose value. When assessing structures, the appropriate indicators should be selected based on the actual circumstances.

Taking into account the current shortcomings in the standards, future improvements and enhancements can be made from three aspects: (a) the establishment of the refined stochastic load model, (b) the analysis of a crowd–structure coupling system, and (c) the modelling of multifactor coupled serviceability evaluation indexes.

Author Contributions: Conceptualization, J.X.; funding acquisition, J.X. and S.D.; methodology, J.X. and S.D.; supervision, H.Q.; writing—original draft, Z.L.; writing—review and editing, Z.L.; validation, H.Q.; resources, H.Q. All authors have read and agreed to the published version of the manuscript.

Funding: This work was supported by the National Natural Science Foundation of China (Grant Nos. 52008376, 51909241 and 52279114) and China Postdoctoral Fund (2023T160200).

Data Availability Statement: New data were created or analyzed in this research. Data will be shared upon request and consideration of the authors.

Conflicts of Interest: The authors declare no conflicts of interest.

References

1. Zeng, D.; Wang, H.; Chen, J. Dynamic reliability analysis of large-span structures under crowd bouncing excitation. *Buildings* **2022**, *12*, 332. [CrossRef]
2. Xiong, J.; Duan, S.; Qian, H.; Pan, Z. Equivalent dynamic load factor of different non-exceedance probability for crowd jumping loads. *Buildings* **2022**, *12*, 450. [CrossRef]
3. Živanovic, S.; Lin, B.; Dang, H.V.; Zhang, S.; Cosic, M.; Caprani, C.; Zhang, Q. Evaluation of inverted-pendulum-with-rigid-legs walking locomotion models for civil engineering applications. *Buildings* **2022**, *12*, 1216. [CrossRef]
4. Wang, Z.; Song, L.; Cheng, Z.; Yang, H.; Wen, J.; Qi, M. Finite element model for vibration serviceability evaluation of a suspended floor with and without tuned mass dampers. *Buildings* **2023**, *13*, 309. [CrossRef]
5. Feng, P.; Wang, Z.; Ji, F.; Zhu, S. Vibration Serviceability Assessment of Pedestrian Bridges Based on Comfort Level. *J. Perform. Constr. Facil.* **2019**, *33*, 04019046. [CrossRef]
6. Strogatz, S.H.; Abrams, D.M.; McRobie, A.; Eckhardt, B.; Ott, E. Crowd synchrony on the Millennium Bridge. *Nature* **2005**, *438*, 43–44. [CrossRef] [PubMed]
7. Muhammad, Z.O.; Reynolds, P. Vibration Serviceability of Building Floors: Performance Evaluation of Contemporary Design Guidelines. *J. Perform. Constr. Facil.* **2019**, *33*, 04019012. [CrossRef]
8. Wang, H.; Ge, Q.; Zeng, D.; Zhang, Z.; Chen, J. Human-Induced Vibration Serviceability: From Dynamic Load Measurement towards the Performance-Based Structural Design. *Buildings* **2023**, *13*, 1977. [CrossRef]
9. Wang, Y.; Ibarra, L.; Pantelides, C. Seismic Retrofit of a Three-Span RC Bridge with Buckling-Restrained Braces. *J. Bridge Eng.* **2016**, *21*, 04016073. [CrossRef]
10. Wang, Y.; Ibarra, L.; Pantelides, C. Collapse capacity of reinforced concrete skewed bridges retrofitted with buckling-restrained braces. *Eng. Struct.* **2019**, *184*, 99–114. [CrossRef]
11. Jafari, M.; Hou, F.; Abdelkefi, A. Wind-induced vibration of structural cables. *Nonlinear Dynam.* **2020**, *100*, 351–421. [CrossRef]
12. Mohamad, H.; Soga, K.; Bennett, P.J. Fibre optic installation techniques for pile instrumentation. In Proceedings of the 17th International Conference on Soil Mechanics and Geotechnical Engineering, Alexandria, Egypt, 5–9 October 2009; pp. 1873–1876.
13. Jusoh, S.N.; Mohamad, H.; Marto, A.; Yunus, N.M.; Kasim, F. Segment's joint in precast tunnel lining design. *J. Teknol.* **2015**, *77*, 91–98. [CrossRef]
14. Živanović, S.; Pavic, A.; Reynolds, P. Vibration serviceability of footbridges under human-induced excitation: A literature review. *J. Sound Vib.* **2005**, *279*, 1–74. [CrossRef]
15. Xiong, J.; Duan, S.; Qian, H.; Pan, Z. Multi-mode response spectrum for multi-harmonic crowd jumping loads. *Appl. Math. Model.* **2022**, *111*, 696–712. [CrossRef]
16. Sheng, P.; Fang, X.; Wen, J.; Yu, D. Vibration properties and optimized design of a nonlinear acoustic metamaterial beam. *J. Sound Vib.* **2021**, *492*, 115739. [CrossRef]
17. Bruno, L.; Corbetta, A. Uncertainties in crowd dynamic loading of footbridges: A novel multi-scale model of pedestrian traffic. *Eng. Struct.* **2017**, *147*, 545–566. [CrossRef]
18. Bruno, L.; Venuti, F. The pedestrian speed-density relation: Modelling and application. In Proceedings of the Third International Conference on Footbridges, Porto, Portugal, 2–4 July 2008.
19. Association Franaise de Génie Civil. *Footbridges-Assessment of Vibrational Behaviour of Footbridges under Pedestrian Loading-Practical Guidelines*; The Sétra: Paris, France, 2006.
20. Research Fund for Coal and Steel. *Design of Footbridges Guidelines*; RFCS: Karlsruhe, Germany, 2007.
21. Croce, P. *Design of Bridges:Guidebook 2*; Czech Technical University: Prague, 2010.
22. International Federation for Structural Concrete. *FIB Bulletin 32: Guidelines for the Design of Footbridges*; FIB: Lausanne, Switzerland, 2006.

23. *ISO 10137*; Bases for Design of Structures—Serviceability of Buildings and Walkways against Vibration. International Organization for Standardization: Geneva, Switzerland, 2007.
24. British Standards Institution. *UK National Annex to Eurocode 1: Actions on Structures-Part 2: Traffic Loads on Bridges. NA to BS EN 1991-2: 2003*; BSI: London, UK, 2008.
25. American Institute of Steel Construction. *Design Guide 11: Vibrations of Steel-Framed Structural Systems Due to Human Activity*; AISC: Chicago, IL, USA, 2016.
26. China Academy of Building Research. *JGJ3-2010: Technical Specification for Concrete Structures of Tall Building*; CABR: Beijing, China, 2010.
27. China Academy of Building Research. *JGJ/T441-2019: Technical Standard for Human Comfort of the Floor Vibration*; CABR: Beijing, China, 2019.
28. Beijing Municipal Engineering Research Institute. *Technical Specifications of Urban Pedestrian Overcrossing and Underpass (Draft for Comments)*; Beijing Municipal Engineering Research Institute: Beijing, China, 2017.
29. Jones, C.A.; Reynolds, P.; Pavic, A. Vibration serviceability of stadia structures subjected to dynamic crowd loads: A literature review. *J. Sound Vib.* **2011**, *330*, 1531–1566. [CrossRef]
30. Cao, L.; Li, J.; Frank Chen, Y.; Huang, S. Measurement and application of walking models for evaluating floor vibration. *Structures* **2023**, *50*, 561–575. [CrossRef]
31. Wang, J.; Chen, J.; Yokoyama, Y.; Xiong, J. Spectral Model for Crowd Walking Load. *J. Struct. Eng.* **2020**, *146*. [CrossRef]
32. Racic, V.; Pavic, A.; Brownjohn, J.M.W. Experimental identification and analytical modelling of human walking forces: Literature review. *J. Sound Vib.* **2009**, *326*, 1–49. [CrossRef]
33. Cuevas, R.G.; Jimenez-Alonso, J.F.; Martinez, F.; Díaz, I.M. Uncertainty-based approaches for the lateral vibration serviceability assessment of slender footbridges. *Structures* **2021**, *33*, 3475–3485. [CrossRef]
34. Bayat, E.; Tubino, F. Human-induced vibrations of floors: A probabilistic approach. *Eng. Struct.* **2024**, *300*, 117198. [CrossRef]
35. Xie, Z.; Hu, X.; Du, H.; Zhang, X. Vibration behavior of timber-concrete composite floors under human-induced excitation. *J. Build. Eng.* **2020**, *32*, 101744. [CrossRef]
36. Wang, J.; Chen, J. A comparative study on different walking load models. *Struct. Eng. Mech.* **2017**, *63*, 847–856. [CrossRef]
37. Van Nimmen, K.; Lombaert, G.; De Roeck, G.; Van den Broeck, P. Vibration serviceability of footbridges: Evaluation of the current codes of practice. *Eng. Struct.* **2014**, *59*, 448–461. [CrossRef]
38. Živanović, S.; Pavic, A.; Ingolfsson, E.T. Modeling Spatially Unrestricted Pedestrian Traffic on Footbridges. *J. Struct. Eng.* **2010**, *136*, 1296–1308. [CrossRef]
39. Živanović, S. *Probability-Based Estimation of Vibration for Pedestrian Structures Due to Walking Type*; University of Sheffield: Sheffield, UK, 2006.
40. Chen, J.; Wang, J.; Brownjohn, J.M.W. Power Spectral-Density Model for Pedestrian Walking Load. *J. Struct. Eng.* **2019**, *145*, 04018239. [CrossRef]
41. Carroll, S.P.; Owen, J.S.; Hussein, M.F.M. Modelling crowd–bridge dynamic interaction with a discretely defined crowd. *J. Sound Vib.* **2012**, *331*, 2685–2709. [CrossRef]
42. Fujino, Y.; Siringoringo, D.M. A Conceptual Review of Pedestrian-Induced Lateral Vibration and Crowd Synchronization Problem on Footbridges. *J. Bridge Eng.* **2016**, *21*, C4015001. [CrossRef]
43. Chen, J.; Xu, R.; Zhang, M. Acceleration response spectrum for predicting floor vibration due to occupant walking. *J. Sound Vib.* **2014**, *333*, 3564–3579. [CrossRef]
44. Chen, J.; Li, G.; Racic, V. Acceleration response spectrum for predicting floor vibration due to occupants jumping. *Eng. Struct.* **2016**, *112*, 71–80. [CrossRef]
45. Brownjohn, J.; Racic, V.; Chen, J. Universal response spectrum procedure for predicting walking-induced floor vibration. *Mech. Syst. Signal Process.* **2016**, *70–71*, 741–755. [CrossRef]
46. Van Nimmen, K.; Lombaert, G.; De Roeck, G.; Van den Broeck, P. The impact of vertical human-structure interaction on the response of footbridges to pedestrian excitation. *J. Sound Vib.* **2017**, *402*, 104–121. [CrossRef]
47. *ISO 2631-1*; Mechanical Vibration and Shock—Evaluation of Human Exposure to Whole-Body Vibration Part 1: General Requirements. ISO: Geneva, Switzerland, 1997.
48. *ISO 2631-2*; Evaluation of Human Exposure to Whole-body Vibration—Part 2: Continous and Shock Induced Vibration in Buildings (1 Hz to 80 Hz). ISO: Geneva, Switzerland, 1989.
49. Garcia-Dieguez, M.; Zapico-Valle, J.L. Statistical modelling of spatiotemporal variability of overground walking. *Mech. Syst. Signal Process.* **2019**, *129*, 186–200. [CrossRef]
50. Garcia-Dieguez, M.; Racic, V.; Zapico-Valle, J.L. Complete statistical approach to modelling variable pedestrian forces induced on rigid surfaces. *Mech. Syst. Signal Process.* **2021**, *159*, 107800. [CrossRef]
51. Mohammed, A.; Pavic, A. Human-structure dynamic interaction between building floors and walking occupants in vertical direction. *Mech. Syst. Signal Process.* **2021**, *147*, 107036. [CrossRef]
52. Lucà, F.; Berardengo, M.; Manzoni, S.; Vanali, M.; Drago, L. Human-structure interaction: Convolution-based estimation of human-induced vibrations using experimental data. *Mech. Syst. Signal Process.* **2022**, *167*, 108511. [CrossRef]
53. Xiong, J.; Chen, J.; Caprani, C. Spectral analysis of human-structure interaction during crowd jumping. *Appl. Math. Model.* **2021**, *89*, 610–626. [CrossRef]

54. Jafry, T. Handbook of Human Vibration—MJ Griffin. *Appl. Ergon.* **1991**, *22*, 270. [CrossRef]
55. Drygala, I.J.; Polak, M.A.; Dulinska, J.M. Vibration serviceability assessment of GFRP pedestrian bridges. *Eng. Struct.* **2019**, *184*, 176–185. [CrossRef]
56. Dong, C.; Bas, S.; Catbas, F.N. Investigation of vibration serviceability of a footbridge using computer vision-based methods. *Eng. Struct.* **2020**, *224*, 111224. [CrossRef]